HHS Public Access

Author manuscript

Cancer Res. Author manuscript; available in PMC 2018 December 15.

Published in final edited form as:

Cancer Res. 2017 December 15; 77(24): 7038–7048. doi:10.1158/0008-5472.CAN-17-2485.

MALT1 inhibition is efficacious in both naïve and ibrutinib-resistant chronic lymphocytic leukemia

Nakhle S. Saba[1], **Deanna H. Wong**[2], **Georges Tanios**[1], **Jessica R. Iyer**[2], **Patricia Lobelle-Rich**[1], **Eman L. Dadashian**[2], **Delong Liu**[2], **Lorena Fontan**[3], **Erik K. Flemington**[4], **Cydney M. Nichols**[2], **Chingiz Underbayev**[2], **Hana Safah**[1], **Ari Melnick**[3], **Adrian Wiestner**[2,*], and **Sarah E. M. Herman**[2,*]

[1]Section of Hematology and Medical Oncology, Department of Medicine, Tulane University, New Orleans, LA

[2]Hematology Branch, National Heart, Lung and Blood Institute, National Institutes of Health, Bethesda, MD

[3]Section of Hematology and Medical Oncology, Department of Medicine, Weill Cornell Medical College, New York, NY

[4]Department of Pathology, Tulane University, New Orleans, LA

Abstract

The clinical efficacy displayed by ibrutinib in chronic lymphocytic leukemia (CLL) has been challenged by the frequent emergence of resistant clones. The ibrutinib target, Bruton's tyrosine kinase (BTK), is essential for B cell receptor signaling, and most resistant cases carry mutations in BTK or PLCG2, a downstream effector target of BTK. Recent findings show that MI-2, a small molecule inhibitor of the para-caspase MALT1, is effective in preclinical models of another type of BCR pathway-dependent lymphoma. We therefore studied the activity of MI-2 against CLL and ibrutinib-resistant CLL. Treatment of CLL cells *in vitro* with MI-2 inhibited MALT1 proteolytic activity, reduced BCR and NF-κB signaling, inhibited nuclear translocation of RelB and p50, and decreased Bcl-xL levels. MI-2 selectively induced dose and time-dependent apoptosis in CLL cells, sparing normal B lymphocytes. Furthermore, MI-2 abrogated survival signals provided by stromal cells and BCR cross-linking and was effective against CLL cells harboring features associated with poor outcomes, including 17p deletion and unmutated IGHV. Notably, MI-2 was effective against CLL cells collected from patients harboring mutations conferring resistance to ibrutinib. Overall, our findings provide a preclinical rationale for the clinical development of MALT1 inhibitors in CLL, in particular for ibrutinib-resistant forms of this disease.

Corresponding Authors: Sarah E. M. Herman, PhD, Hematology Branch, National Heart Lung and Blood Institute (NHLBI), National Institutes of Health (NIH), Building 10 CRC 3E-5232, 10 Center Drive, Bethesda, MD 20892-1202, Phone: (301) 496-5328, Sarah.Herman@nih.gov; Nakhle S. Saba, MD, Section of Hematology & Medical Oncology, Tulane University, 1430 Tulane Ave, SL-78, New Orleans, LA 70112, Phone: (504) 988-6234, nsaba@tulane.edu.

*Wiestner A and Herman S.E.M contributed equally to this work

Conflict of Interest: Dr. Wiestner received research funding from Pharmacyclics. All other authors declare no conflict of interest.

Keywords

CLL; MALT1; MI-2; ibrutinib; B-cell receptor

Introduction

Activation of B-cell receptor (BCR) and NF-κB pathways within the lymph node (LN) microenvironment are critical for CLL proliferation and survival (1). High rates of clinical response in patients treated with kinase inhibitors validate the therapeutic targeting of these pathways in CLL (2-6). Ibrutinib covalently binds to and irreversibly inhibits Bruton's tyrosine kinase (BTK), an essential kinase for BCR signaling (2,7,8). Objective response rates with single-agent ibrutinib are as high as 70% in relapsed or refractory patients and can reach 86% in first line therapy (2,7). Equally high initial response rates have been reported in patients with deletion 17p (8,9). However, patients with deletion 17p, especially those with relapsed or refractory disease, have shorter progression free survival than patients without these high-risk features (10,11). In fact, more than half of all patients with previously treated CLL enrolled in the phase Ib/II trial suffered disease progression within 5 years on ibrutinib, and patients with 17p deletion had a median progression free survival of 26 months (12). In the NIH cohort, median progression free survival was 38.8 months in patients with high-risk disease in either the treatment-naïve or relapsed settings (13). High risk is defined by having a TP53 aberration and a Rai stage III/IV (in previously-treated patients) in addition to a β2-microglobulin >4 (in previously-untreated patients) (13). The most common findings in patients resistant to ibrutinib are non-synonymous mutations affecting the cysteine 481 (C481) of BTK, which forms a covalent bond with ibrutinib, and gain of function mutations in PLCγ2 downstream of BTK. Other less frequent genetic alterations have been associated with ibrutinib resistance, including 8p deletion (10,14-16). Ibrutinib-resistant CLL can progress rapidly and effective treatment options are limited (11,17,18). Objective responses following progression on ibrutinib have been observed with the BCL2 antagonist venetoclax and the PI3Kδ inhibitor idelalisib (19).

The paracaspase *mucosa-associated lymphoid tissue lymphoma translocation 1* (MALT1) was first identified as the fusion partner in the translocation t(11;18)(q21;q21) found in a subset of mucosa-associated lymphoid tissue (MALT) lymphoma. MALT lymphomas typically arise as antigen-driven lymphomas and can remit after an inciting infection is eradicated. The chromosomal translocation creates the API2-MALT1 fusion oncoprotein that promotes antigen-independent MALT1 activation and NF-κB signaling (20). MALT1 is the enzymatically active component of the CARD11-BCL10-MALT1 (CBM) signaling complex (21). The gatekeeper role of the CBM complex is also evidenced by CARD11 mutations that are oncogenic drivers in a subset of activated B-cell-like diffuse large B-cell lymphoma (ABC-DLBCL) (22). Furthermore, recurrent gain-of- function germ line variants in RNF31, a component of the linear ubiquitin chain assembly complex that cooperates with CBM to activate NF-κB, has been implicated in lymphomagenesis (23).

Given its oncogenic role in lymphomas, targeting MALT1 has been pursued as a therapeutic strategy (24-28). MI-2 ($C_{19}H_{17}Cl_3N_4O_3$) covalently binds to C464 within the paracaspase

domain of MALT1 and thereby suppresses its protease activity (24). Fontan and colleagues showed that MI-2 irreversibly inhibits the cleavage of MALT1 substrates in ABC-DLBCL cell lines, thereby reducing constitutive NF-κB pathway activity and cell proliferation and survival (24). In contrast, germinal center B-cell-like (GCB)-DLBCL, which lacks constitutive NF-κB activation, was not sensitive (24,29). At least in mice, MI-2 was so far well-tolerated and not associated with specific toxicities (24).

The possible therapeutic role of MI-2 in CLL, has not been investigated. We hypothesized that MALT1 inhibition could have anti-leukemic activity in CLL. Further, given that most mutations associated with ibrutinib resistance reactivate NF-κB signaling upstream of MALT1, we hypothesize that targeting MALT1 could be effective in ibrutinib-resistant CLL.

Materials and Methods

Patients and samples

Peripheral blood mononuclear samples (PBMCs) were obtained from treatment-naïve and relapsed CLL patients (Supplementary Tables S1-2). Written informed consent in accordance with the Declaration of Helsinki was obtained overseen by Institutional Review Boards at Tulane University (New Orleans, LA; #M0600) and at the NHLBI (NCT00923507). PBMCs were isolated using density gradient centrifugation with lymphocyte separation medium (ICN Biomedicals). Fresh cells were subjected to CD19 selection using magnetic beads yielding purity >96% (Miltenyi Biotec). As previously described, *IGHV* sequencing was performed on leukemic samples and classified as mutated (<98% homology to germline) or unmutated (≥98% homology) (30). In select experiments we utilized clinical samples collected from patients with CLL treated with single agent ibrutinib on a phase 2 trial (NCT01500733) at baseline, on treatment (12 months) and at clinical progression. MEC1 cell line was originally purchased from DSMZ expanded *in vitro*, then viably frozen using strict conditions to prevent microbial- and cross-contaminations. Cells were then used within 3 weeks of thawing. MEC1 was derived from a patient with CLL in prolymphocytoid transformation.

Cell viability assay

CellTiter 961 AQueous One Solution Reagent (Promega) MTS dye reduction assay was used to quantify cell viability. Cells were incubated for 24 or 48h with MI-2 (0-50 μM) in a 96-well plate at 500 000 cells/well. At the end of the incubation period, MTS was added and incubated for 1-4h at 37°C. The absorbance was measured using a 96-well plate reader. MI-2 was kindly provided by Dr. Ari Melnick (Weill Cornell Medical College, New York), or purchased from Selleckchem.

Flow cytometry

PBMCs were treated with various concentrations MI-2 or DMSO (control) in the presence or absence of 100 μM of the pan-caspase inhibitor z-VAD-fmk (R&D Systems). Cells were stained with anti- Annexin-V, and CD19 (BD Biosciences), ViViD Live-Dead stain, and/or TO-PRO-3 stain (Invitrogen), and analyzed by flow cytometry as previously described (31).

In select experiments cells were stained for the activation markers CD69 and CD86 (BD Biosciences).

Immunoblot

Immunoblot experiments were carried out as previously described (32). Primary antibodies used were anti: MALT1 (cat #2494) and anti-c-PARP (Asp214; cat#9541), t-PARP (cat#9532s), GAPDH (cat#2118S), Bcl-xL (cat#2764S), all from Cell Signaling Technology; CYLD (cat#sc-137139) and Actin (cat#sc-47778), both from Santa Cruz Biotechnology. Secondary antibodies used were: IRDye goat anti-rabbit (cat#926-68071), IRDye goat anti-mouse (cat#926-32210), both from LI-COR Biosciences or ECL donkey anti-rabbit IgG HRP (GE healthcare). The signal was visualized using Odyssey Imaging System (LI-COR Biosciences) or LAS-4000 imaging system (Fuji Film).

Assessment of the protective effect of the Microenvironment

Primary CLL cells were co-cultured in the presence or absence of nurse-like cells (NLC) or 5 μg/ml of anti-Human IgM (Jackson ImmunoResearch, Cat#109-006-129), with or without MI-2, for 24h (33). CLL cell viability was determined by flow cytometry using TO-PRO-3.

RNA sequencing and gene expression analysis

Total RNA was extracted from CLL PBMC's using RNeasy kit (Qiagen), and cDNA was prepared using the High Capacity cDNA RT Kit (Applied Biosystems). NF-κB specific gene signature score was determined as previously described (34). Briefly, expression of six NF-κB target genes was quantified by real-time polymerase chain reaction (RT-PCR) on TaqMan Primers on an ABI PRISM 7900HT Sequence Detection System (Applied Biosystems). The difference in threshold cycle (ΔCt) for each gene of interest was calculated from the Ct of the housekeeping gene (VCP)—Ct of the gene of interest (e.g., CCL3). The ΔCt for the pathway-specific genes (six unique genes for NF-κB) were averaged into a signature score.

MI-2-treated and untreated PBMCs were purified by CD19 selection and subjected to RNA sequencing as previously described (35). Briefly, polyadenylated RNA was enriched by two rounds of oligo(dT) selection (Invitrogen), followed by library construction and paired-end sequencing of 50bp reads on Illumina HiSeq-2000. We used MapSplice 2 to map RNA-seq reads to human genome hg19, Samtools package (DHIGroup) to remove duplicate reads and create mpileup files, and VarScan package (Genome Institute, Washington University) for INDEL and single-nucleotide variant callings. Variants were annotated using ANNOVAR. RNA sequencing data are deposited in GEO under accession number GSE98206.

NF-κB activity assay

NF-κB activity was measured using the TransAM NF-κB transcription factor assay kit (Active Motif). CLL PBMC's were treated with or without MI-2 (2.5 and 5μM) for 6h. Nuclear lysates were extracted via Nuclear Extract Kit (Active Motif). Nuclear lysates were applied to 96-well plates coated with oligonucleotides containing NF-κB consensus sequence (5′-GGGACTTTCC-3′). The change in expression of RelB and p50 isoforms were determined by comparing samples to matched untreated controls.

Droplet Digital PCR

Droplet digital PCR (ddPCR) was performed on DNA isolated from stored samples after $CD19^+$ selection, as described previously (36). Briefly, custom ddPCR assays were obtained from Bio-Rad Laboratories and analyzed using a Bio-Rad QX200 droplet reader. Each mutation detection assay was run duplexed to a matched wild-type assay (primer and probe sequences, Supplementary Table S3) in quadruplicates. Variant allele frequencies (VAFs) were calculated from the fraction of positive droplets with a reported sensitivity of 0.01%.

Statistical analysis

The Student *t* test (paired or unpaired), Fisher's exact test, and one-way analysis of variance were used to assess the differences between groups. All *P* values were 2-sided and values ≤ .05 were considered statistically significant. For RT-PCR data, the raw Ct value was normalized to internal control. Analyses were performed using GraphPad Prism (GraphPad Software Inc), JMP software (SAS Institute), and R statistical software 3.2.2 (Institute for Statistics and Mathematics).

Results

MALT1 is more active in CLL compared to normal B cells

We first sought to determine the protein expression patterns of MALT1 in primary CLL cells and normal B cells. To this end, we used immunoblot assays to compare MALT1 protein levels in CD19-selected CLL cells collected from 21 patients, and in B cells of six normal volunteers. We found that MALT1 protein expression was highly variable in CLL, and lower than in normal B cells on average (Fig. 1A-B).

In order to determine whether MALT1 is active in CLL, we measured cleaved CYLD in freshly isolated primary CLL cells and normal B cells. CYLD is a direct target of MALT1, and the degree of CYLD cleavage reflects MALT1 activity (37). We used immunoblotting with an antibody specific for the C-terminal (C-ter) region of CYLD, to detect full length CYLD (120 kDa) and the C-ter cleaved product ($CYLD^{C\text{-}ter}$ ~70KDa) (38). While $CYLD^{C\text{-}ter}$ was present in most CLL samples, almost no expression was detected in normal B cells, indicating that MALT1-dependent proteolysis is ongoing in CLL *in vivo*, but not in normal B cells (Fig. 1A,C).

Inhibition of MALT1 with MI-2 induced dose- and time-dependent apoptosis in CLL cells

We first evaluated effects of MI-2 in MEC1 cells. MI-2 dose-dependently reduced cell viability, with an inhibitory concentration 50% (IC_{50}) at 24h of 0.2 μM (Supplementary Fig. S1A), consistent with previously published data in sensitive DLBCL cell lines (IC_{50}, 0.2-0.5 μM) (24). Next, we tested PBMCs from 22 CLL patients against serial dilutions of MI-2 for 24h. All samples showed dose-dependent responses (Fig. 2A), with a mean IC_{50} of 1.17 μM and a 95% confidence interval (95% CI) of 0.79 to 1.74 μM. To assess cytotoxicity against CLL cells specifically, we measured the viability of CLL cells (CD19-positive) by flow cytometry using Annexin-V and ViViD Live-Dead stain. We observed a dose- and time-dependent increase in CLL cell death following exposure to MI-2 for 24 and 48h (Fig. 2B, Supplementary Fig. S1B). The mechanism of cell killing appears to be primarily through

apoptosis as evident by the dose dependent increase in both the Annexin-V-positive fraction of CLL cells (Fig. 2B) and increased PARP cleavage (Fig. 2C). Consistently, the pan caspase inhibitor z-VAD-fmk inhibited PARP cleavage (Fig. 2D) and reduced MI-2-induced cell death by 55 to 64% (Supplementary Fig. S1C).

To determine MI-2 toxicity for normal B, we exposed PBMCs from five healthy volunteers to increasing concentrations of MI-2 for 24h. A statistically significant increase in cell death was observed only at 10 μM in CD19+ cells from normal donors (Supplementary Fig. S1D). Taken together, MI-2 is preferentially cytotoxic for CLL cells compared to normal B lymphocytes (Supplementary Fig. S1E).

MI-2 thwarts the protective effect of the microenvironment in CLL

Next, we used the NLC co-culture system or anti-IgM mediated BCR activation to determine whether MI-2 can overcome tumor-microenvironment interactions or antigen stimulation (33,39). To this end, we treated primary CLL cells cultured in the presence or absence of NLC (N=5) or after IgM activation (N=4) with MI-2 (0.5-4 μM) for 48h. Co-culture with NLC or with anti-IgM improved the viability of the untreated primary CLL samples *in vitro* (Fig. 3A-C). Despite this, MI-2 remained effective against CLL cells in the presence of NLC and BCR crosslinking (Fig. 3A-C). Akin to ibrutinib, we observed a reduction in MI-2 cell-killing ability at low concentrations (≤ 2 μM) in the presence of NLC compared to the no-NLC group (40). However, NLC loses their protective effects when MI-2 is used at 4 μM (Supplementary Fig. S2A). In comparison, BCR crosslinking did not provide any protective effects against MI-2 for any of the concentrations used (Supplementary Fig. S2B). Further, there was no cytotoxic effect on NLC at any of the used concentrations of MI-2 (measured by MTS assay, data not shown).

We next sought to investigate whether disease heterogeneity is a driving factor in MI-2 sensitivity. We characterized our samples for *IGHV* mutational status, 17p deletion, prior treatment status and CD38 expression. With the exception of slightly increased sensitivity of *IGHV* mutated samples at 2.5 μM, treatment with MI-2 was equally active against CLL cells regardless of 17p deletion status, prior therapy status, or CD38 expression (Supplementary Fig. S2C-F).

MI-2 inhibits NF-κB signaling and disrupts a myriad of biological networks in CLL

In ABC-DLBCL cell lines, 8h of MALT1 inhibition effectively inhibited expression of NF-κB-regulated genes (24,28). To investigate the effect of MI-2 on CLL tumor biology, RNA from purified CLL cells treated for 8h with 2 μM MI-2 *in vitro* (N=3) was subject to RNA sequencing and compared to untreated controls (N=3). Out of 24,462 tested genes, there were 438 genes whose expression changed ≥2-fold at $P<0.05$ (312 down- and 126 up-regulated) (Fig. 4A, Supplementary Table S4).

To identify the biologic basis for the MI-2-induced changes in gene expression, we chose Gene Set Enrichment Analysis (GSEA) as an investigator-independent discovery tool (41). GSEA identified 35 *Hallmark* and *Oncogenic Signatures* gene sets that were differentially enriched between the treated samples compared to their control counterparts at FDR ≤ 5%, and normalized enrichment score (NES) ≥ 1.50. Of these, 32 gene sets relevant to CLL, were

grouped based on their functional similarities into two distinct categories (Supplementary Table S5): “Signaling/Interaction with the Microenvironment” including BCR and NF-κB signaling pathways; and “Proliferation/Malignancy”, all were downregulated by MI-2. Collectively, GSEA clearly identified the BCR and NF-κB pathways among the top affected pathways (Fig. 4B-C, Supplementary Table S5).

To confirm the inhibition of the canonical NF-κB pathway, we assessed the expression of six known NF-κB target genes (*CCND2*, *BCL2A*, *CCL3*, *CCL4*, *RGS1*, and *TNF*) (1) by quantitative RT-PCR in CLL cells following a 6h exposure to MI-2 at 2.5 and 5 μM. As a quantitative measure of NF-κB signaling, we computed a gene signature score as the averaged expression of these six genes. Expression of all six genes was significantly reduced following exposure to MI-2, which translates into reduction in the signature score (Fig. 4D), therefore reflecting an effective inhibition of the NF-κB pathway.

MI-2 inhibits CYLD cleavage, suppresses NF-κB translocation to the nucleus, and restores apoptosis in CLL

Cleavage of CYLD is ongoing in CLL and represents direct *in vivo* evidence of the proteolytic activity of MALT1 (Fig. 1A,C). To investigate the direct effect of MI-2 on MALT1 proteolytic activity, we measured the effect of MI-2 on CYLD cleavage, and detected a clear reduction in the level of cleaved CYLD (Fig. 5A).

MALT1 has been implicated in both canonical and non-canonical NF-κB signaling (21,42). To evaluate the impact of MI-2 on canonical and non-canonical NF-κB activation, we used ELISA to measure the nuclear levels of p50 and RelB, respectively. Indeed, treatment with MI-2 resulted in a statistically significant, dose-dependent reduction of both p50 (Fig. 5B) and RelB (Fig. 5C) nuclear levels. Consistently, we observed decreased expression of the activation markers CD69 and CD86 on the surface of CLL cells following treatment with MI-2 (Fig. 5D). Similarly, the protein level of Bcl-xL, an anti-apoptotic protein whose expression is transcriptionally controlled by NF- κB (43), was reduced in cells treated with MI-2 (Fig. 5E).

MI-2 is effective against ibrutinib-resistant CLL cells

A treatment-induced lymphocytosis at the start of therapy with kinase inhibitors is well appreciated and does not cause morbidity or predict inferior outcome (11,44). While most patients have resolution of lymphocytosis within the first year, a subset of patients have persistent lymphocytosis for years raising concerns about the risk of acquired resistance (44). We sought to determine whether MI-2 can overcome “ibrutinib-tolerance” in these cells. We therefore collected PBMCs from CLL patients having an absolute lymphocyte count >10,000 cells/μL at one year from the start of ibrutinib and within 4-12 hours of their last dose of ibrutinib (on-treatment sample) and compared their drug sensitivity to matched samples obtained before the start of ibrutinib (baseline sample) (Supplementary Fig. S3A). The IC_{50} of MI-2 against on-treatment samples was 2.5 μM, comparable to the IC_{50} previously determined for ibrutinib naïve samples (Fig. 6A). In a head-to-head comparison of patient-matched baseline and on-treatment samples, the sensitivity to MI-2 in the on-treatment samples appeared slightly increased compared to baseline (Fig. 6B).

To test the activity of MI-2 in ibrutinib-resistant disease, we exposed PBMCs collected from patients who progressed on ibrutinib to increasing concentrations of MI-2 *in vitro*. These samples were collected either at the time of relapse while remaining on ibrutinib, or after the drug was stopped but prior to initiation of another therapy. CLL cells collected at the time of progression were sensitive to MI-2 treatment (Fig. 6C). As reported, most cases of ibrutinib resistance in our patients were associated with mutations in *BTK* and/or *PLCG2* (10). We found that cells collected from patients with a mutation in either one of these genes (or both) were sensitive to MI-2 with IC_{50} values comparable to baseline samples (N=8, Supplementary Fig. S3B). However, cells from patients with an unknown resistance driver tended to be less sensitive to MI-2 (Supplementary Fig. S3B). Where possible we tested MI-2 effects against samples from patients at baseline, on-treatment, and at progression and found that they were equally sensitive to MI-2 (Fig. 6D). Since resistance mutations may be present in a minority of the cell population at progression (10), we sought to assess the effect of MI-2 specifically against mutant subclones. We therefore treated samples with known *BTK* and/or *PLCG2* mutations with 5μM of MI-2 for 24h and determined the variant allele frequency (VAF) of mutated *BTK* (C481S) or *PLCG2* (R665W or L845F) in purified tumor cells using a digital PCR assay. Following treatment with MI-2, CLL cells in two out of three patients with a *BTK* mutation showed a significant reduction in VAF suggesting that mutated cells were more sensitive to MALT1 inhibition than the cells with wild type BTK (Fig. 6E). In the third patient, there was no difference. VAFs of *PLCG2* mutations was low and did not change with MI-2 treatment, suggesting that both the mutated and unmutated cells responded equally to MI-2 treatment *in vitro* (Fig. 6E).

Discussion

Progressive CLL develops in about half of high-risk patients during the first 3 years on ibrutinib and is the leading cause of death for these patients (10,15). Thus, novel therapeutic strategies are needed to regain disease control in patients progressing on ibrutinib. Here we show that the paracaspase MALT1 is a promising target in CLL, particularly for ibrutinib-resistant disease. We show for the first time that MALT1 is constitutively active in CLL, and that targeting MALT1 with MI-2 is effective against ibrutinib-resistant tumor cells. MI-2 was equally effective against CLL cells activated through the BCR or cultured in the presence of NLC or having adverse genetic features such as unmutated *IGHV* and 17p deletion. Further, MI-2 was selectively toxic for CLL cells, while sparing non-malignant B cells. Like ibrutinib, MI-2 potently inhibited BCR and NF-κB signaling. In contrast to ibrutinib, MI-2 induced apoptosis, which could result in deeper clinical responses.

MALT1 and the CBM complex connect antigen signaling to NF-κB activation. Oncogenic lesions that activate CBM confer antigen-independent NF-κB activation in lymphoma (20,22). In CLL MALT1 appears constitutively activated, likely as part of BCR signaling, and is turned off by MI-2. Most known ibrutinib resistance mutations reactivate BCR signaling upstream of MALT1. Thus, targeting MALT1 provides an opportunity to overcome the effects of BTK and PLCG2 mutations at the next critical junction in signal transduction. Basal activity of MALT1 in CLL is evident by the higher level of CYLD cleavage detected in comparison to normal B-cells. Consistent with increased protease activity, including autocleavage (45), MALT1 levels are lower in CLL compared to normal B-cells. Similar

observations were described by Dai and colleagues who detected lower levels of MALT1 and higher levels of cleaved CYLD in mantle cell lymphoma cell lines with active MALT1 compared to cell lines with inactive MALT1 (25). Other MALT1 targets include A20, BCL10, and RELB (21,28).

Reduced CYLD cleavage and inhibition of NF-κB signaling in primary CLL cells by MI-2 is consistent with data in lymphoma cell lines (24,25). However, our transcriptome analysis in CLL cells treated with MI-2 revealed not only the expected downregulation of NF-κB target genes but suggested a broader impact of the drug, including inhibition of the JAK-STAT, interferon, and Ras signaling pathways (46,47). NF-κB inhibition is reflected in decreased levels of nuclear p50 and RelB, and select NF-κB regulated molecules, in particular Bcl-xL. MALT1 has been implicated in both canonical and non-canonical NF-κB signaling, and its absence has been shown to impair B cell activation factor (BAFF)-mediated translocation of RelB into the nucleus in MALT1$^{-/-}$ B cells, consistent with our data (42).

Direct induction of apoptosis distinguishes MI-2 from BCR inhibitors, particularly ibrutinib which promotes little apoptosis even when used at high concentrations (48-50). Like ibrutinib, MI-2 was equally effective against cells with or without adverse characteristics such as unmutated *IGHV* and 17p deletion. MI-2 also abrogated the survival support of NLC and anti-IgM crosslinking, microenvironmental stimuli that support CLL survival *in vivo* and that can promote resistance to chemotherapy as well as novel agents (51,52). The pan-caspase inhibitor Z-VAD-fmk rescued cells from MI-2-induced cytotoxicity consistent with induction of apoptosis due to MALT1 inhibition. Notably, the MALT1 protease cleaves substrates after Arg, while caspases cleave after Asp, and is not affected by Z-VAD fmk (21).

Despite recent improvements, the management of progressive disease on BCR inhibitors remains challenging (53). The median survival for patients progressing on ibrutinib with CLL is around 2 years, and even shorter for Richter's transformation (10,15,17). Objective responses with venetoclax following ibrutinib failure have been achieved in 70%. However, complete remissions were seen in only 2% (18), likely predicting for short duration of response based on prior studies with venetoclax (54). There is less experience with the PI3Kδ idelalisib in this setting and the overall response rate at 28% is lower (55). While mutations in CARD11 have been associated with ibrutinib resistance in diffuse large B cell lymphoma, CARD11 mutations are uncommon in CLL. Notably, MI-2 restored sensitivity to ibrutinib in CARD11 mutant cells, and induced CARD11 degradation resulting in NF-κB inhibition (27). Mutations in MALT1 or in elements downstream to MALT1 have not been described as causes of ibrutinib resistance, suggesting that targeting MALT1 could overcome resistance. In agreement, we show that MI-2 remained active in ibrutinib-resistant disease and that subclones harboring mutations in *BTK* and/or *PLCG2* were at least as sensitive as their wildtype counterparts. These results also suggest that MI-2 might overcome resistance to other BTK inhibitors in CLL, such as acalabrutinib whose mechanisms of resistance also appear to be mediated by mutations in *BTK* and/or *PLCG2* (3). Interestingly, “ibrutinib-tolerant” cells that persisted for 12 months or more in patients on treatment were more sensitive to MI-2 compared to matching cells collected prior to starting ibrutinib, suggesting

that the two drugs might act synergistically, providing a rationale to explore concurrent targeting of BTK and MALT1.

In conclusion, these data identify MALT1 as an outstanding therapeutic candidate for ibrutinib-resistant CLL. MALT1 inhibitors should be investigated in clinical trials for patients progressing on BCR inhibitors.

Supplementary Material

Refer to Web version on PubMed Central for supplementary material.

Acknowledgments

We thank our patients for participating and donating the blood and tissue samples to make this research possible. We thank Melody Baddoo and the members of the Cancer Genetics Program - COBRE core at Tulane University for assistance with gene expression profiling and RNA sequencing analysis. We also thank the Louisiana Cancer Research Center (LCRC) bio-specimen core for their help in blood sample collection and processing.

Financial Support: This work was funded by the Hope Foundation SWOG Early Exploration and Development (SEED) Program (Grant# RS15SEED; Primary recipient, Nakhle Saba) and the Intramural Research Program of the National Heart, Lung, and Blood Institute, National Institutes of Health (Grant# ZIA HL002346-13; Primary recipient, Adrian Wiestner).

References

1. Herishanu Y, Perez-Galan P, Liu D, Biancotto A, Pittaluga S, Vire B, et al. The lymph node microenvironment promotes B-cell receptor signaling, NF-kappaB activation, and tumor proliferation in chronic lymphocytic leukemia. Blood. 2011; 117:563–74. [PubMed: 20940416]
2. Byrd JC, Furman RR, Coutre SE, Flinn IW, Burger JA, Blum KA, et al. Targeting BTK with ibrutinib in relapsed chronic lymphocytic leukemia. N Engl J Med. 2013; 369:32–42. [PubMed: 23782158]
3. Byrd JC, Harrington B, O'Brien S, Jones JA, Schuh A, Devereux S, et al. Acalabrutinib (ACP-196) in Relapsed Chronic Lymphocytic Leukemia. N Engl J Med. 2016; 374:323–32. [PubMed: 26641137]
4. Friedberg JW, Sharman J, Sweetenham J, Johnston PB, Vose JM, Lacasce A, et al. Inhibition of Syk with fostamatinib disodium has significant clinical activity in non-Hodgkin lymphoma and chronic lymphocytic leukemia. Blood. 2010; 115:2578–85. [PubMed: 19965662]
5. Furman RR, Sharman JP, Coutre SE, Cheson BD, Pagel JM, Hillmen P, et al. Idelalisib and Rituximab in Relapsed Chronic Lymphocytic Leukemia. New England Journal of Medicine. 2014; 370:997–1007. [PubMed: 24450857]
6. Wiestner A. The role of B-cell receptor inhibitors in the treatment of patients with chronic lymphocytic leukemia. Haematologica. 2015; 100:1495–507. [PubMed: 26628631]
7. Burger JA, Tedeschi A, Barr PM, Robak T, Owen C, Ghia P, et al. Ibrutinib as Initial Therapy for Patients with Chronic Lymphocytic Leukemia. New England Journal of Medicine. 2015; 373:2425–37. [PubMed: 26639149]
8. Farooqui MZ, Valdez J, Martyr S, Aue G, Saba N, Niemann CU, et al. Ibrutinib for previously untreated and relapsed or refractory chronic lymphocytic leukaemia with TP53 aberrations: a phase 2, single-arm trial. The Lancet Oncology. 2015; 16:169–76. [PubMed: 25555420]
9. O'Brien S, Jones JA, Coutre SE, Mato AR, Hillmen P, Tam C, et al. Ibrutinib for patients with relapsed or refractory chronic lymphocytic leukaemia with 17p deletion (RESONATE-17): a phase 2, open-label, multicentre study. Lancet Oncol. 2016; 17:1409–18. [PubMed: 27637985]
10. Ahn IE, Underbayev C, Albitar A, Herman SEM, Tian X, Maric I, et al. Clonal evolution leading to ibrutinib resistance in chronic lymphocytic leukemia. Blood. 2017; 129:1469–79. [PubMed: 28049639]

11. Byrd JC, Furman RR, Coutre SE, Burger JA, Blum KA, Coleman M, et al. Three-year follow-up of treatment-naive and previously treated patients with CLL and SLL receiving single-agent ibrutinib. Blood. 2015; 125:2497–506. [PubMed: 25700432]
12. O'Brien SM, Furman RR, Coutre SE, Flinn IW, Burger J, Blum K, et al. Five-Year Experience with Single-Agent Ibrutinib in Patients with Previously Untreated and Relapsed/Refractory Chronic Lymphocytic Leukemia/Small Lymphocytic Leukemia. Blood. 2016; 128:233.
13. Ahn IE, Tian X, Soto S, Valdez J, Lotter J, Farooqui M, et al. Prognostic Models Predictive of Disease Progression in CLL Patients Treated with Ibrutinib. Blood. 2016; 128:187.
14. Lenz G. Deciphering Ibrutinib Resistance in Chronic Lymphocytic Leukemia. J Clin Oncol. 2017; 35:1451–2. [PubMed: 28291389]
15. Woyach JA, Ruppert AS, Guinn D, Lehman A, Blachly JS, Lozanski A, et al. BTKC481S-Mediated Resistance to Ibrutinib in Chronic Lymphocytic Leukemia. Journal of Clinical Oncology. 2017; 35:1437–43. [PubMed: 28418267]
16. Burger JA, Landau DA, Taylor-Weiner A, Bozic I, Zhang H, Sarosiek K, et al. Clonal evolution in patients with chronic lymphocytic leukaemia developing resistance to BTK inhibition. Nat Commun. 2016; 7:11589. [PubMed: 27199251]
17. Jain P, Keating M, Wierda W, Estrov Z, Ferrajoli A, Jain N, et al. Outcomes of patients with chronic lymphocytic leukemia after discontinuing ibrutinib. Blood. 2015; 125:2062–7. [PubMed: 25573991]
18. Jones J, Choi MY, Mato AR, Furman RR, Davids MS, Heffner LT, et al. Venetoclax (VEN) Monotherapy for Patients with Chronic Lymphocytic Leukemia (CLL) Who Relapsed after or Were Refractory to Ibrutinib or Idelalisib. Blood. 2016; 128:637.
19. Mato AR, Nabhan C, Barr PM, Ujjani CS, Hill BT, Lamanna N, et al. Outcomes of CLL patients treated with sequential kinase inhibitor therapy: a real world experience. Blood. 2016; 128:2199–205. [PubMed: 27601462]
20. Sagaert X, De Wolf-Peeters C, Noels H, Baens M. The pathogenesis of MALT lymphomas: where do we stand? Leukemia. 2007; 21:389–96. [PubMed: 17230229]
21. Coornaert B, Baens M, Heyninck K, Bekaert T, Haegman M, Staal J, et al. T cell antigen receptor stimulation induces MALT1 paracaspase-mediated cleavage of the NF-kappaB inhibitor A20. Nat Immunol. 2008; 9:263–71. [PubMed: 18223652]
22. Lenz G, Davis RE, Ngo VN, Lam L, George TC, Wright GW, et al. Oncogenic CARD11 mutations in human diffuse large B cell lymphoma. Science. 2008; 319:1676–9. [PubMed: 18323416]
23. Yang Y, Schmitz R, Mitala J, Whiting A, Xiao W, Ceribelli M, et al. Essential role of the linear ubiquitin chain assembly complex in lymphoma revealed by rare germline polymorphisms. Cancer discovery. 2014; 4:480–93. [PubMed: 24491438]
24. Fontan L, Yang C, Kabaleeswaran V, Volpon L, Osborne MJ, Beltran E, et al. MALT1 small molecule inhibitors specifically suppress ABC-DLBCL in vitro and in vivo. Cancer cell. 2012; 22:812–24. [PubMed: 23238016]
25. Dai B, Grau M, Juilland M, Klener P, Horing E, Molinsky J, et al. B-cell receptor-driven MALT1 activity regulates MYC signaling in mantle cell lymphoma. Blood. 2017; 129:333–46. [PubMed: 27864294]
26. Ferch U, Kloo B, Gewies A, Pfander V, Duwel M, Peschel C, et al. Inhibition of MALT1 protease activity is selectively toxic for activated B cell-like diffuse large B cell lymphoma cells. The Journal of experimental medicine. 2009; 206:2313–20. [PubMed: 19841089]
27. Xue L, Apatira M, Sirisawad M, Chang B. Abstract 1742: Ibrutinib plus proteasome or MALT1 inhibitors overcome resistance to BCR antagonists in CARD11 mutant-expressing B-lymphoma cells. Cancer research. 2015; 75:1742.
28. Hailfinger S, Lenz G, Ngo V, Posvitz-Fejfar A, Rebeaud F, Guzzardi M, et al. Essential role of MALT1 protease activity in activated B cell-like diffuse large B-cell lymphoma. Proc Natl Acad Sci U S A. 2009; 106:19946–51. [PubMed: 19897720]
29. Wilson WH, Young RM, Schmitz R, Yang Y, Pittaluga S, Wright G, et al. Targeting B cell receptor signaling with ibrutinib in diffuse large B cell lymphoma. Nat Med. 2015; 21:922–6. [PubMed: 26193343]

30. Wiestner A, Rosenwald A, Barry TS, Wright G, Davis RE, Henrickson SE, et al. ZAP-70 expression identifies a chronic lymphocytic leukemia subtype with unmutated immunoglobulin genes, inferior clinical outcome, and distinct gene expression profile. Blood. 2003; 101:4944–51. [PubMed: 12595313]
31. Fiskus W, Saba N, Shen M, Ghias M, Liu J, Gupta SD, et al. Auranofin induces lethal oxidative and endoplasmic reticulum stress and exerts potent preclinical activity against chronic lymphocytic leukemia. Cancer Res. 2014; 74:2520–32. [PubMed: 24599128]
32. Saba NS, Angelova M, Lobelle-Rich PA, Levy LS. Disruption of pre-B-cell receptor signaling jams the WNT/beta-catenin pathway and induces cell death in B-cell acute lymphoblastic leukemia cell lines. Leukemia research. 2015; 39:1220–8.
33. Burger JA, Tsukada N, Burger M, Zvaifler NJ, Dell'Aquila M, Kipps TJ. Blood-derived nurse-like cells protect chronic lymphocytic leukemia B cells from spontaneous apoptosis through stromal cell-derived factor-1. Blood. 2000; 96:2655–63. [PubMed: 11023495]
34. Herman SE, Mustafa RZ, Gyamfi JA, Pittaluga S, Chang S, Chang B, et al. Ibrutinib inhibits BCR and NF-kappaB signaling and reduces tumor proliferation in tissue-resident cells of patients with CLL. Blood. 2014; 123:3286–95. [PubMed: 24659631]
35. Saba NS, Liu D, Herman SE, Underbayev C, Tian X, Behrend D, et al. Pathogenic role of B-cell receptor signaling and canonical NF-kappaB activation in mantle cell lymphoma. Blood. 2016; 128:82–92. [PubMed: 27127301]
36. Wong TN, Ramsingh G, Young AL, Miller CA, Touma W, Welch JS, et al. Role of TP53 mutations in the origin and evolution of therapy-related acute myeloid leukaemia. Nature. 2015; 518:552–5. [PubMed: 25487151]
37. Ginster S, Bardet M, Unterreiner A, Malinverni C, Renner F, Lam S, et al. Two Antagonistic MALT1 Auto-Cleavage Mechanisms Reveal a Role for TRAF6 to Unleash MALT1 Activation. PLoS One. 2017; 12:e0169026. [PubMed: 28052131]
38. Douanne T, Gavard J, Bidere N. The paracaspase MALT1 cleaves the LUBAC subunit HOIL1 during antigen receptor signaling. Journal of cell science. 2016; 129:1775–80. [PubMed: 27006117]
39. Guarini A, Chiaretti S, Tavolaro S, Maggio R, Peragine N, Citarella F, et al. BCR ligation induced by IgM stimulation results in gene expression and functional changes only in IgV H unmutated chronic lymphocytic leukemia (CLL) cells. Blood. 2008; 112:782–92. [PubMed: 18487510]
40. Primo D, De la Serna J, Martinez J, González M, Lopez J, Bárez A, et al. Development of a High-Throughput Screening Assay with Nurse-like Cell-Based Microenviroment in Chronic Lymphoid Leukemia Cells. Blood. 2014; 124:3639.
41. Subramanian A, Tamayo P, Mootha VK, Mukherjee S, Ebert BL, Gillette MA, et al. Gene set enrichment analysis: a knowledge-based approach for interpreting genome-wide expression profiles. Proc Natl Acad Sci U S A. 2005; 102:15545–50. [PubMed: 16199517]
42. Tusche MW, Ward LA, Vu F, McCarthy D, Quintela-Fandino M, Ruland J, et al. Differential requirement of MALT1 for BAFF-induced outcomes in B cell subsets. The Journal of experimental medicine. 2009; 206:2671–83. [PubMed: 19917778]
43. Lee HH, Dadgostar H, Cheng Q, Shu J, Cheng G. NF-kappaB-mediated up-regulation of Bcl-x and Bfl-1/A1 is required for CD40 survival signaling in B lymphocytes. Proc Natl Acad Sci U S A. 1999; 96:9136–41. [PubMed: 10430908]
44. Herman SE, Niemann CU, Farooqui M, Jones J, Mustafa RZ, Lipsky A, et al. Ibrutinib-induced lymphocytosis in patients with chronic lymphocytic leukemia: correlative analyses from a phase II study. Leukemia. 2014; 28:2188–96. [PubMed: 24699307]
45. Baens M, Bonsignore L, Somers R, Vanderheydt C, Weeks SD, Gunnarsson J, et al. MALT1 auto-proteolysis is essential for NF-kappaB-dependent gene transcription in activated lymphocytes. PLoS One. 2014; 9:e103774. [PubMed: 25105596]
46. Wang L, Kurosaki T, Corey SJ. Engagement of the B-cell antigen receptor activates STAT through Lyn in a Jak-independent pathway. Oncogene. 2007; 26:2851–9. [PubMed: 17146444]
47. Hashimoto A, Okada H, Jiang A, Kurosaki M, Greenberg S, Clark EA, et al. Involvement of guanosine triphosphatases and phospholipase C-gamma2 in extracellular signal-regulated kinase,

c-Jun NH2-terminal kinase, and p38 mitogen-activated protein kinase activation by the B cell antigen receptor. J Exp Med. 1998; 188:1287–95. [PubMed: 9763608]

48. Herman SE, Gordon AL, Hertlein E, Ramanunni A, Zhang X, Jaglowski S, et al. Bruton tyrosine kinase represents a promising therapeutic target for treatment of chronic lymphocytic leukemia and is effectively targeted by PCI-32765. Blood. 2011; 117:6287–96. [PubMed: 21422473]
49. Hoellenriegel J, Coffey GP, Sinha U, Pandey A, Sivina M, Ferrajoli A, et al. Selective, novel spleen tyrosine kinase (Syk) inhibitors suppress chronic lymphocytic leukemia B-cell activation and migration. Leukemia. 2012; 26:1576–83. [PubMed: 22362000]
50. Herman SE, Gordon AL, Wagner AJ, Heerema NA, Zhao W, Flynn JM, et al. Phosphatidylinositol 3-kinase-delta inhibitor CAL-101 shows promising preclinical activity in chronic lymphocytic leukemia by antagonizing intrinsic and extrinsic cellular survival signals. Blood. 2010; 116:2078–88. [PubMed: 20522708]
51. Vogler M, Butterworth M, Majid A, Walewska RJ, Sun XM, Dyer MJ, et al. Concurrent up-regulation of BCL-XL and BCL2A1 induces approximately 1000-fold resistance to ABT-737 in chronic lymphocytic leukemia. Blood. 2009; 113:4403–13. [PubMed: 19008458]
52. Davids MS, Deng J, Wiestner A, Lannutti BJ, Wang L, Wu CJ, et al. Decreased mitochondrial apoptotic priming underlies stroma-mediated treatment resistance in chronic lymphocytic leukemia. Blood. 2012; 120:3501–9. [PubMed: 22955911]
53. Woyach JA. How I manage ibrutinib-refractory chronic lymphocytic leukemia. Blood. 2017; 129:1270–4. [PubMed: 28096090]
54. Roberts AW, Davids MS, Pagel JM, Kahl BS, Puvvada SD, Gerecitano JF, et al. Targeting BCL2 with Venetoclax in Relapsed Chronic Lymphocytic Leukemia. New England Journal of Medicine. 2016; 374:311–22. [PubMed: 26639348]
55. Porcu P, Flinn I, Kahl BS, Horwitz SM, Oki Y, Byrd JC, et al. Clinical Activity of Duvelisib (IPI-145), a Phosphoinositide-3-Kinase-δ,γ Inhibitor, in Patients Previously Treated with Ibrutinib. Blood. 2014; 124:3335.

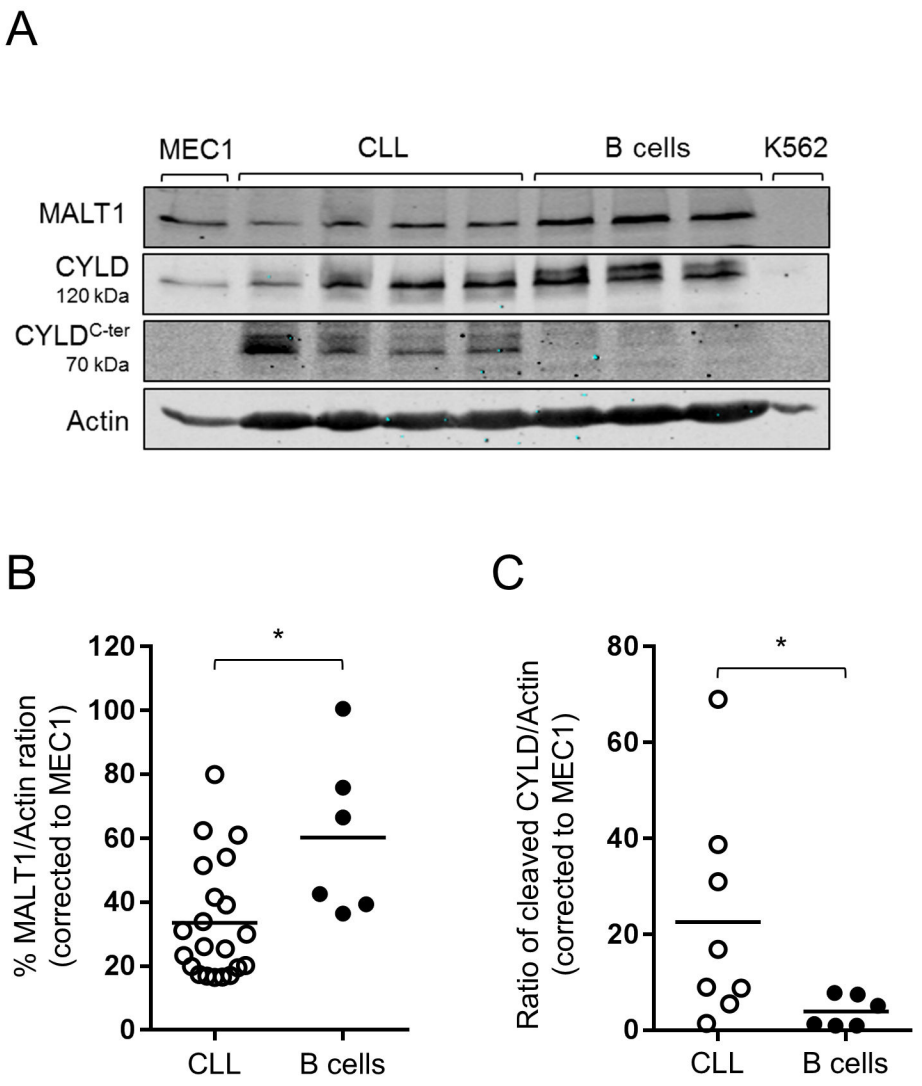

Figure 1. MALT1 is constitutively active in CLL

(A) A representative Immunoblot analysis of MALT1, CYLD, and the C-terminal cleaved form of CYLD (CYLD$^{C\text{-}ter}$ a 70kDa CYLD cleavage product) in CD19-selected primary CLL samples and normal B cells. MEC1 and K562 were used as positive and negative controls, respectively. Actin is shown as a loading control. (B) MALT1 protein levels shown as % MALT1/Actin in CLL (N=21) and normal B cells (N=6) measured by immunoblot as described in (A), normalized using MALT1/Actin ratio of MEC1 across different experiments. (C) Cleaved CYLD (CYLD$^{C\text{-}ter}$) protein levels shown as CYLD$^{C\text{-}ter}$/Actin in CLL (N=8) and normal B cells (N=6) measured by immunoblot as described in (A), normalized using CYLD$^{C\text{-}ter}$/Actin ratio of MEC1 across different experiment. Comparisons in (B) and (C) were conducted using unpaired Student *t* test.

*, $P<0.05$.

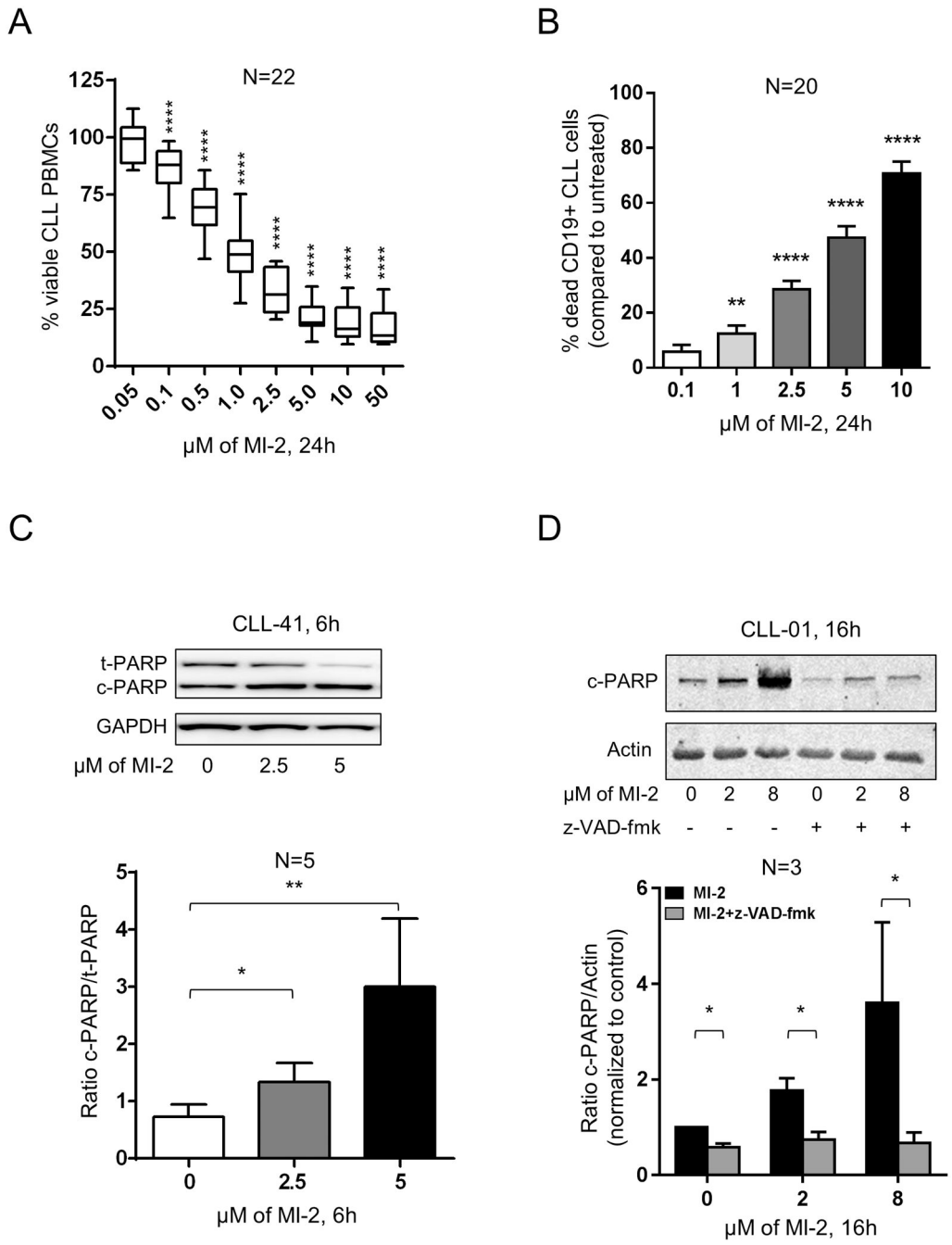

Figure 2. Targeting MALT1 with MI-2 results in dose- and time-dependent apoptotic cell death in CLL

(A) PBMCs from 22 patients with CLL were incubated in duplicates with increasing concentrations of MI-2 for 24h. Cell viability was quantified using MTS assay and shown as % of untreated control. (B) Percent dead CD19-gated CLL cells (CD19+/Annexin-V+/ViViD+; N=20) relative to untreated control is shown after 24h treatment with MI-2. Error bars represent SEM. (C) A representative immunoblot showing the change in expression of total and cleaved PARP (t-PARP and c-PARP, respectively) in purified CLL cells (CD19-selected) following a 6h exposure to 2.5 and 5 µM of MI-2. GAPDH is shown as a loading

control. Ratio of c-PARP/t-PARP (± SEM) of purified CLL cells collected from 5 patients following treatment with MI-2. Error bars represent SEM. (D) A representative immunoblot showing the change in expression of c-PARP in purified CLL cells following a 16h exposure to 2 and 8 μM of MI-2 in the presence or absence of z-VAD-fmk. Actin is shown as a loading control. Ratio of c-PARP/Actin (± SEM) of purified CLL cells collected from three individual patients following treatment with MI-2 (+/-z-VAD-fmk). Error bars represent SEM.

SEM, standard error of mean; -, absence; +, presence; NS, non-significant; ND, normal donor; *, $P<0.05$; **, $P<0.01$; ****, $P<0.0001$.

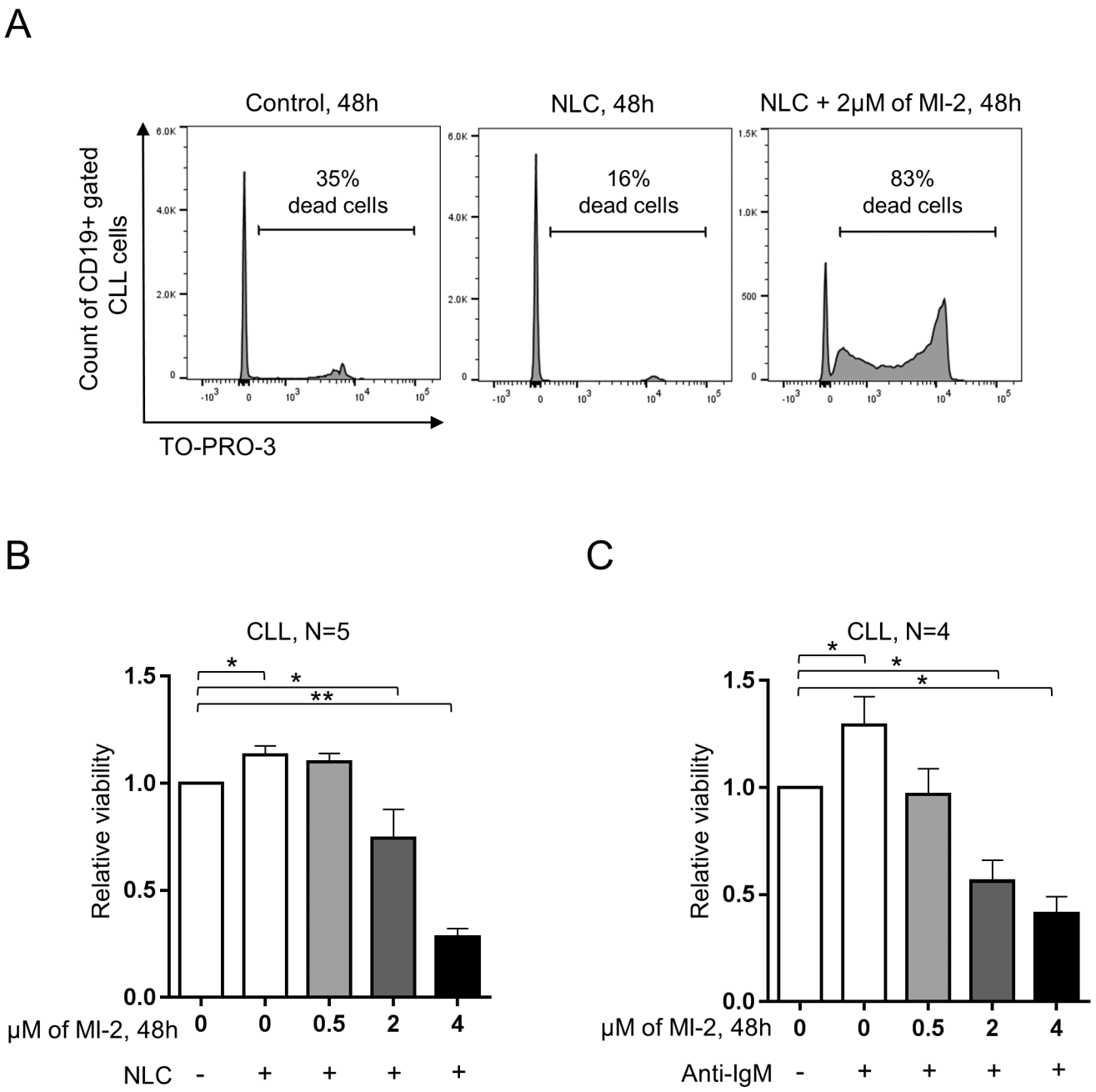

Figure 3. MI-2 overcomes the protective effect of the microenvironment

(A) A representative flow panel showing the increase in cell death (TO-PRO-3 stained) in CD19 gated CLL cells, following exposure to 2 μM of MI-2 for 48h in the presence or absence of NLC. (B) PBMCs of 5 patients with CLL were incubated for 48h with 0, 0.5, 2, and 4 μM of MI-2 in the presence or absence of NLC. Shown is the viability of CD19 gated CLL cells as in (A). (C) Purified CLL cells (CD19 selection) (N=4) were incubated for 48h with 0, 0.5, 2, and 4 μM of MI-2 in the presence or absence of 5 μg/ml of anti-IgM. Shown is the CLL cells viability relative to untreated control without anti-IgM, measured by MTS. Error bars represent SEM.

SEM, standard error of mean; NLC, nurse-like cells; -, absence; +, presence; *, $P<0.05$; **, $P<0.01$.

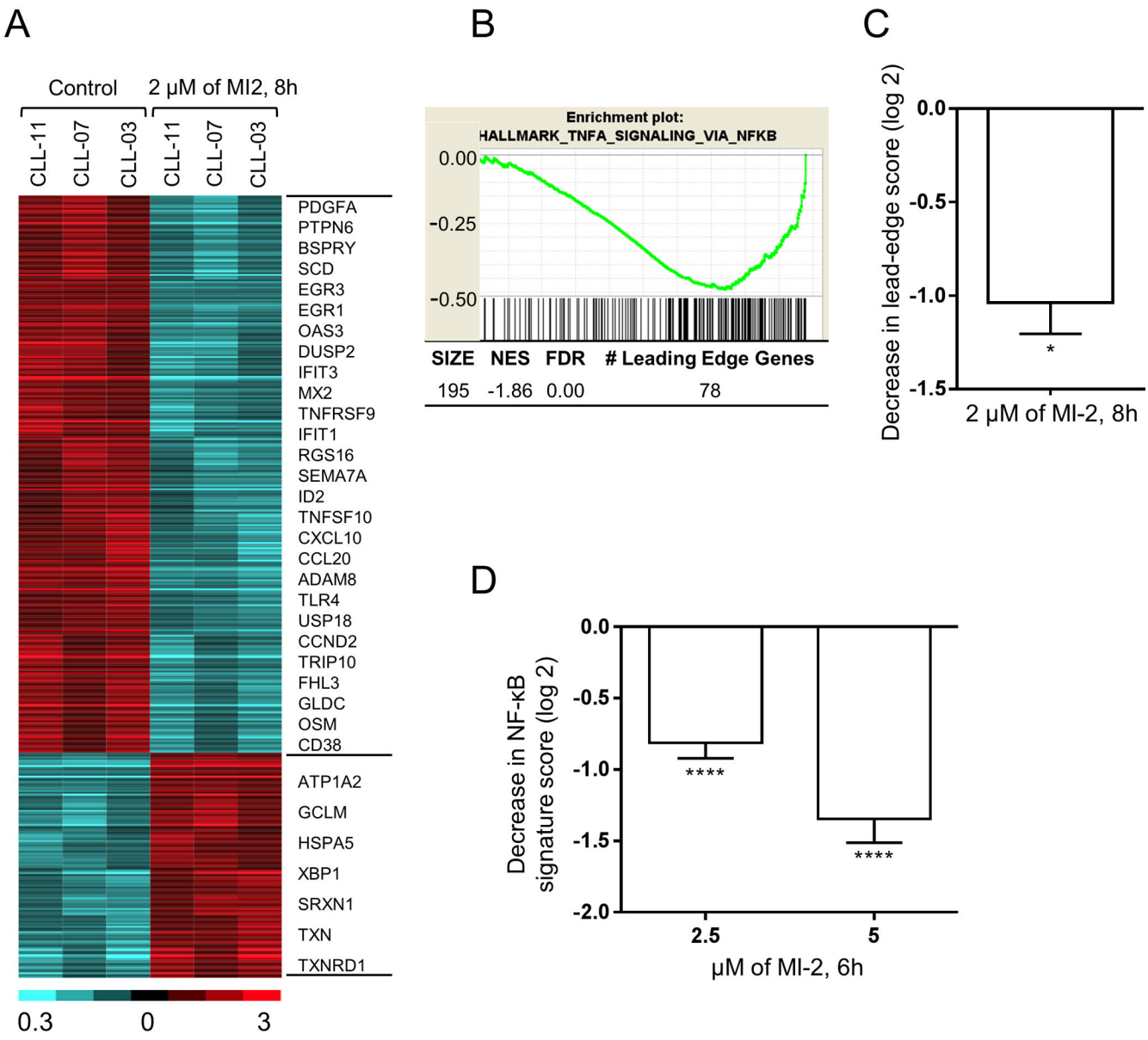

Figure 4. MI-2 inhibits NF-κB signaling and disrupts multiple biologic networks in CLL

(A) RNA gene expression analysis of CD19-selected CLL cells treated with 2 μM MI-2 for 8h was performed by RNA sequencing. The heatmap represents 438 genes whose expression changed ≥2-fold at $P<0.05$ (312 down- and 126 up-regulated). Gene expression is median-centered and scaled as indicated. Each column represents a sample, and each row represents a gene. Gene symbols highlight select genes. (B) A representative enrichment plot showing the inhibitory effect of MI-2 on an NF-κB gene set identified by GSEA. (C) Decrease in the "signature score" of this NF-κB gene set is shown on the right, and was computed as the average of the mRNA expression level of the "leading edge genes" of MI-2-treated samples minus corresponding control. The "leading edge genes" represent the genes of this NF-κB gene set most significantly differentially expressed in the experimental data, as determined by GSEA. (D) Average NF-κB signature score (± SEM) of six NF-κB target genes across

ten CD19-selected samples following treatment with 2.5 or 5 μM of MI-2 for 6h normalized to untreated expression.

*, $P<0.05$; ****, $P<0.0001$; NES, normalized enrichment score; FDR, false discovery rate; SEM, standard error of mean.

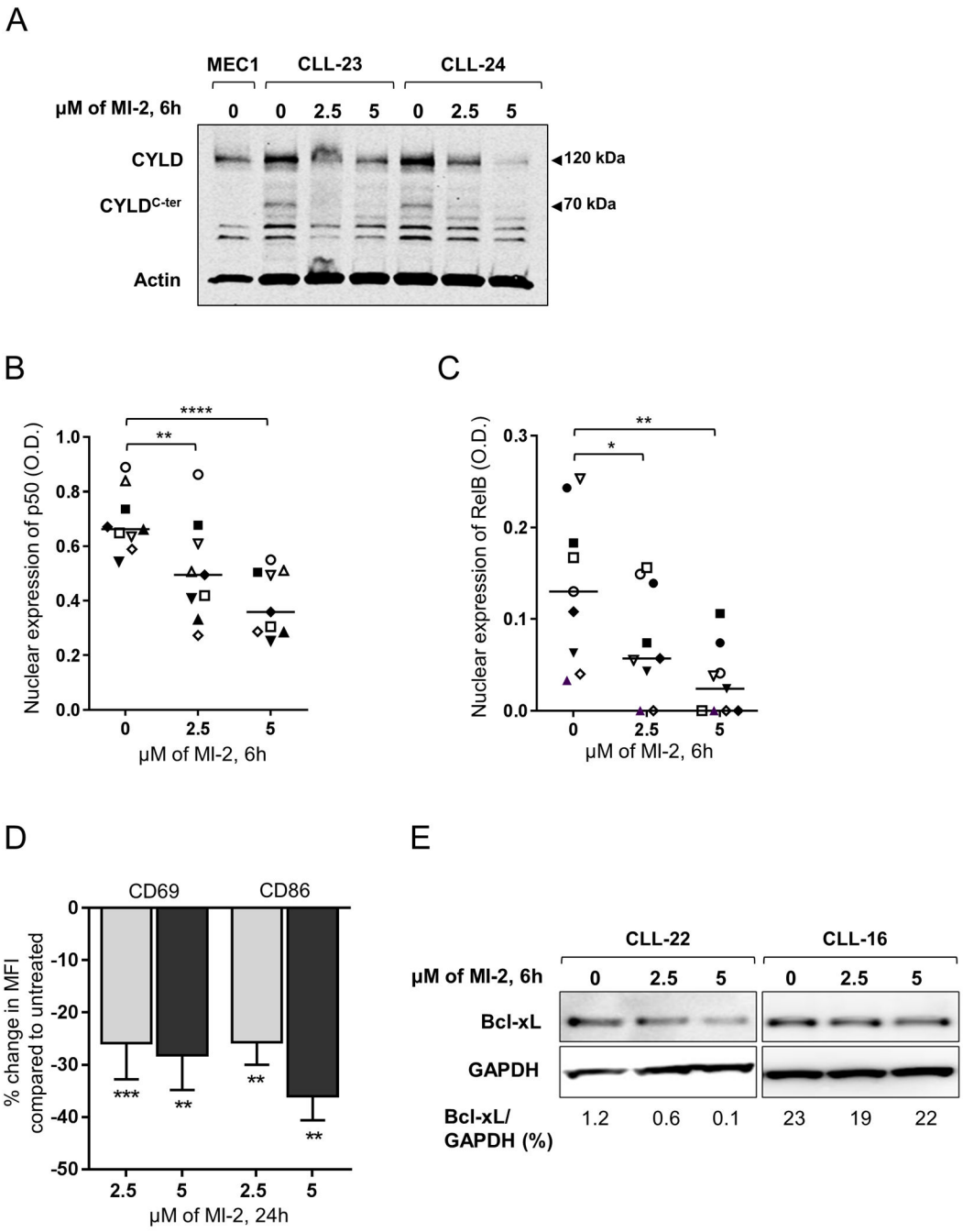

Figure 5. MI-2 inhibits CYLD cleavage, suppresses NF-κB translocation to the nucleus, and restores apoptosis in CLL

(A) Immunoblot assay of whole cell lysates extracted from CD19-selected CLL cells collected from two patients showing the changes in total CYLD (120 kDa), and cleaved CYLD ($CYLD^{C\text{-}ter}$, 70 kDa) following a 6h exposure to 2.5 and 5 μM of MI-2. Actin is shown as a loading control. (B, C) Nuclear expression of NF-κB subunits (B) p50 and (C) RelB determined by ELISA (N=9) following a 6h exposure to 2.5 and 5 μM of MI-2. Each patient is represented by a unique symbol; lines represent median values. (D) Primary CLL PBMC's (N=13) were incubated with or without 2.5 μM or 5 μM MI-2 for 24h. Shown is the

% change in MFI in CD19+ CLL cells for activation markers CD69 and CD86 normalized to untreated control. (E) Immunoblot of two CLL patients showing change in Bcl-xL expression following a 6h exposure to 2.5 and 5 μM MI-2. All comparisons by paired Student *t* test.

*, $P<0.05$; **, $P<0.01$; ****, $P<0.0001$.

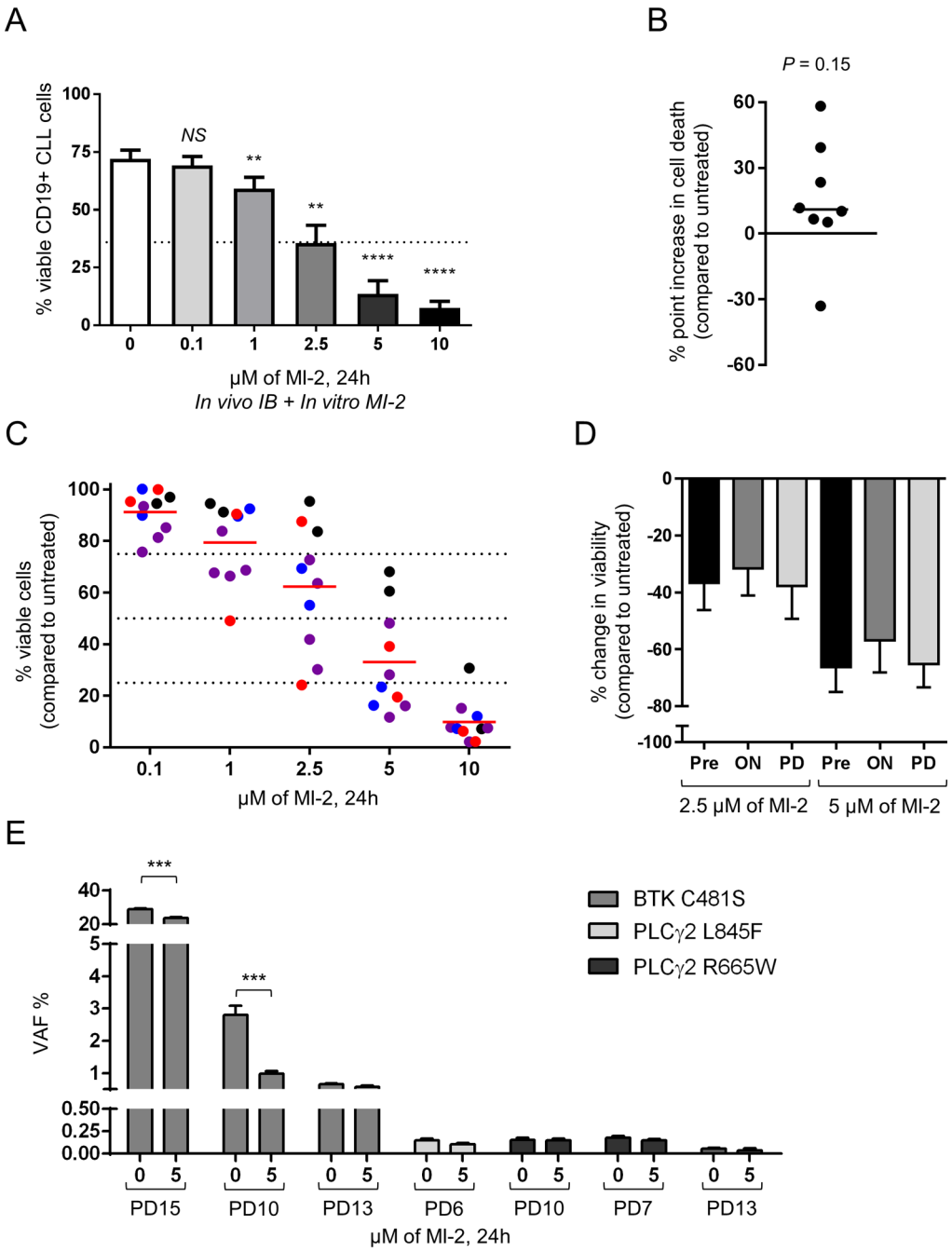

Figure 6. MI-2 is effective against ibrutinib-resistant CLL

(A) Primary CLL PBMCs collected from patients treated for 12 months with ibrutinib were incubated with or without MI-2 at 0-10 μM. Mean ±SEM % viable CLL cells (CD19+/ Annexin-V-/ViViD-) is shown after 24h of MI-2 treatment (N=10). (B) % point difference in cell death of CLL cells from patients on ibrutinib compared to pre-treatment is shown after 24h exposure to 2.5 μM MI-2 *in vitro* (N=8). (C) PBMCs collected from CLL patients with acquired ibrutinib resistance were incubated with or without MI-2. % viable CLL cells (CD19+/Annexin-V-/ViViD-) is shown after 24h exposure to increasing concentrations of

MI-2 relative to untreated control (N=10). Red symbols represent samples with BTK mutations, blue symbols represent PLCγ2 mutations, purple symbols represent samples with both BTK and PLCγ2 mutations, and black symbols represent patients with no known resistance mutations. (D) Mean ±SEM % change in viable CLL cells (CD19+/Annexin-V-/ViViD-) collected from patients prior to treatment (Pre), on *in vivo* ibrutinib (ON) and after progressing on ibrutinib (PD) is shown after 24h exposure to 2.5 μM of MI-2 relative to time matched untreated control (N=7). (E) Variant allele frequency (VAF) in samples from patients shown in (C) with BTK C481S mutations or PLCγ2 R665W or L845F mutations left untreated or exposed to 5 μM MI-2 for 24h (N=7) is shown.
NS, non-significant; **, $P<0.01$; ***, $P<0.001$; ****, $P<0.0001$. SEM, standard error of mean.